Synchrosqueezing-based time-frequency analysis of multivariate data

Alireza Ahrabian [a], David Looney [a], Ljubiša Stanković [a,b], Danilo P. Mandic [a,*]

[a] Department of Electrical and Electronic Engineering, Imperial College London, United Kingdom
[b] Department of Electrical Engineering, University of Montenegro, Montenegro

ABSTRACT

The modulated oscillation model provides physically meaningful representations of time-varying harmonic processes, and has been instrumental in the development of modern time-frequency algorithms, such as the synchrosqueezing transform. We here extend this concept to multivariate signals, in order to identify oscillations common to multiple data channels. This is achieved by introducing a multivariate extension of the synchrosqueezing transform, and using the concept of joint instantaneous frequency multivariate data. For rigor, an error bound which assesses the accuracy of the multivariate instantaneous frequency estimate is also provided. Simulations on both synthetic and real world data illustrate the advantages of the proposed algorithm.

© 2014 Elsevier B.V. All rights reserved.

1. Introduction

Numerous observations in science and engineering exhibit time-varying oscillatory behavior that is not possible to characterize adequately by conventional Fourier analysis. This limitation was first addressed by the modulated oscillation model [1], which characterizes time-varying signals as amplitude and frequency modulated oscillations, thereby capturing the changing oscillatory dynamics of the signal. The univariate modulated oscillation model has since become a standard in analyzing time-varying signals, in fields ranging from communication theory [2] to biomedical engineering [3].

The notion of the univariate modulated oscillation has been recently extended to both bivariate and trivariate time-varying signals [4–6]; in the bivariate case the modulated oscillations are modeled as tracing an ellipse with the joint instantaneous frequency capturing the combined frequencies of the individual channels. This elliptic (ellipsoid) characterization has found applications in oceanography [7], where the underlying physical processes are well modeled as particles in 2D and 3D spaces which trace elliptical trajectories. For an arbitrary number of channels, the modulated multivariate oscillation has been proposed in [8,9], whereby the underlying model assumes one common oscillation that best fits all of the individual channel oscillations. For instance, the work in [9] identifies modulated multivariate oscillations using the multivariate extension of the wavelet ridge algorithm, a local optimization technique that identifies local maxima with respect to scale parameter in the wavelet coefficients, with the objective of extracting the local oscillatory dynamics of the signal. It should be noted that interest in time-frequency analysis of multichannel data has also recently been growing with multivariate data driven algorithms [10,11] that directly exploit multichannel interdependencies.

A recent class of time-frequency techniques, referred to as reassignment methods [12–14], aim to improve the "readability" (localization) of time-frequency representations [15].

The synchrosqueezing transform (SST) [16,17] belongs to this class, it is a post-processing technique based on the continuous wavelet transform that generates highly localized time-frequency representations of nonlinear and nonstationary signals. Synchrosqueezing provides a solution that mitigates the limitations of linear projection based time-frequency algorithms, such as the short-time Fourier transform (STFT) and continuous wavelet transforms (CWT). The synchrosqueezing transform reassigns the energies of these transforms, such that the resulting energies of coefficients are concentrated around the instantaneous frequency curves of the modulated oscillations. As such, synchrosqueezing is an alternative to the recently introduced empirical mode decomposition (EMD) algorithm [18]; it builds upon the EMD, by generating localized time-frequency representations while at the same time providing a well understood theoretical basis.

However, despite all those efforts, multivariate time-frequency algorithms are still at their infancy. This is in stark contrast with the developments in sensor technology which have made readily accessible multivariate data (3D inertial body sensor and 3D anemometers). To this end, we develop a multivariate time-frequency algorithm based on SST that generates a compact time-frequency representation of multichannel signals, based on the principles developed in [8,9,19].

The organization of this paper is as follows: Section 2 introduces the notion of modulated multivariate oscillations and joint instantaneous frequency. Section 3 describes the SST, Section 4 presents the proposed multivariate extension of the synchrosqueezing algorithm, and Section 5 verifies the algorithm through simulations.

2. Modulated multivariate oscillations

Signals containing single time varying amplitudes and frequencies are readily described by the modulated oscillation model

$$x(t) = a(t) \cos \phi(t) \tag{1}$$

where $a(t)$ and $\phi(t)$ are respectively the instantaneous amplitude and phase, and are termed the canonical pair [2]. The application of the Hilbert transform to the original signal, yields the analytic signal $x_+(t)$ in the form

$$x_+(t) = a(t)e^{i\phi(t)} = x(t) + i\mathcal{H}\{x(t)\} \tag{2}$$

where $\mathcal{H}\{\cdot\}$ is the Hilbert transform operator, and $i = \sqrt{-1}$. The analytic signal $x_+(t)$ is complex valued and admits a unique time-frequency representation for the signal $x(t)$, based on the derivative of the instantaneous phase, $\phi(t)$.

Recently, the concept of univariate modulated oscillation has been extended to the multivariate case, in order to model the joint oscillatory structure of a multichannel signal, using the well understood concepts of joint instantaneous frequency and bandwidth. Extending the representation in (2), for multichannel signal $\mathbf{x}(t)$, we can construct a vector at each time instant t, to give a multivariate analytic signal

$$\mathbf{x}_+(t) = \begin{bmatrix} a_1(t)e^{i\phi_1(t)} \\ a_2(t)e^{i\phi_2(t)} \\ \vdots \\ a_N(t)e^{i\phi_N(t)} \end{bmatrix} \tag{3}$$

where $a_n(t)$ and $\phi_n(t)$ represent the instantaneous amplitude and phase for each channel $n = 1, ..., N$. The work in [9] proposed the joint instantaneous frequency (power weighted average of the instantaneous frequencies of all the channels) of multivariate data in the form:

$$\omega_x(t) = \frac{\Im\left\{\mathbf{x}_+^H(t)\dfrac{d}{dt}\mathbf{x}_+(t)\right\}}{\|\mathbf{x}_+(t)\|^2} = \frac{\sum_{n=1}^{N} a_n^2(t)\phi_n'(t)}{\sum_{n=1}^{N} a_n^2(t)} \tag{4}$$

where the symbol "$\Im$" denotes the imaginary part of a complex signal and $\phi_n'(t)$ is the instantaneous frequency for each channel.

Remark 1. It should be noted that for single channel multicomponent signals, the weighted average instantaneous frequency [20] has the same form as in (4) and is consistent with the joint instantaneous frequency.

Both measures of instantaneous frequency overcome a fundamental problem that arises when estimating instantaneous frequency of multiple modulated oscillations, that is, power imbalances between the components lead to instantaneous frequency estimates that are outside the bounds of the individual instantaneous frequencies [21].

The joint instantaneous frequency captures the combined oscillatory dynamics of multivariate signals, while the joint instantaneous bandwidth $v_x(t)$ captures the deviations of the multivariate oscillations in each channel from the joint instantaneous frequency, and is given by

$$v_x(t) = \frac{\left\|\dfrac{d}{dt}\mathbf{x}_+(t) - i\omega_x(t)\mathbf{x}_+(t)\right\|}{\|\mathbf{x}_+(t)\|}. \tag{5}$$

Therefore, the joint instantaneous bandwidth represents the normalized error of the joint instantaneous frequency estimate with respect to the rate of change of the multivariate analytic signal $\mathbf{x}_+(t)$. Inserting (3) into (5) results in the expression for the squared instantaneous bandwidth:

$$v_x^2(t) = \frac{\sum_{n=1}^{N} (a_n'(t))^2 + \sum_{n=1}^{N} a_n^2(t)(\phi_n'(t) - \omega_x(t))^2}{\sum_{n=1}^{N} a_n^2(t)}. \tag{6}$$

Remark 2. Observe that the instantaneous bandwidth depends upon the rate of change of the instantaneous amplitudes for each channel, as well as the deviation of the instantaneous frequencies in each channel from the combined joint instantaneous frequency. Large deviations of the individual instantaneous frequencies from the joint instantaneous frequency result in a large instantaneous bandwidth, implying that the multivariate signal would not be well modeled as a multivariate modulated oscillation.

It has been shown in [6] that the global moments of the joint analytic spectrum can be expressed in terms of the joint instantaneous frequency and bandwidth. The first and second global moments are termed the joint mean frequency and the joint global second central moments (multivariate bandwidth squared). As a result, given the

joint analytic spectrum

$$S(\omega) = \frac{1}{E} \| \mathbf{X}_+(\omega) \|^2, \qquad (7)$$

where $\mathbf{X}_+(\omega)$ is the Fourier transform of $\mathbf{x}_+(t)$ and E is the total energy of the Fourier coefficients given by

$$E = \frac{1}{2\pi} \int_0^\infty \| \mathbf{X}_+(\omega) \|^2 \, d\omega, \qquad (8)$$

this makes possible to express the joint global mean frequency expressed as the first moment of the joint analytic spectrum as

$$\overline{\omega} = \frac{1}{2\pi} \int_0^\infty \omega S(\omega) \, d\omega. \qquad (9)$$

The joint global second central moment (multivariate bandwidth squared) measures the spectral deviation of the joint analytic spectrum from the joint global mean frequency, and is given by

$$\overline{\sigma}^2 = \frac{1}{2\pi} \int_0^\infty (\omega - \overline{\omega})^2 S(\omega) \, d\omega. \qquad (10)$$

Accordingly, the global moments of the analytic spectrum can be related to the moments of joint instantaneous frequency and bandwidth as

$$\overline{\omega} = \frac{1}{E} \int_{-\infty}^\infty \| \mathbf{x}_+(t) \|^2 \omega_x(t) \, dt \qquad (11)$$

$$\overline{\sigma}^2 = \frac{1}{E} \int_{-\infty}^\infty \| \mathbf{x}_+(t) \|^2 \sigma_x^2(t) \, dt, \qquad (12)$$

where $\sigma_x^2(t)$ is the joint instantaneous second central moment, given by

$$\sigma_x^2(t) = v_x^2(t) + (\omega_x(t) - \overline{\omega})^2. \qquad (13)$$

Remark 3. Observe that the multivariate bandwidth squared, $\overline{\sigma}^2$, depends on both the joint instantaneous bandwidth, $\sigma_x^2(t)$, and the deviations of the joint instantaneous frequency from the joint global mean frequency, $\overline{\omega}$.

3. Synchrosqueezing transform

The synchrosqueezing transform is a post-processing technique applied to the continuous wavelet transform in order to generate localized time-frequency representations of non-stationary signals. The continuous wavelet transform is a projection based algorithm that identifies oscillatory components of interest through a series of time-frequency filters known as wavelets. A wavelet $\psi(t)$ is a finite oscillatory function, which when convolved with a signal $x(t)$, in the form

$$W(a, b) = \int a^{-1/2} \psi\left(\frac{t-b}{a}\right) x(t) \, dt \qquad (14)$$

gives the wavelet coefficients $W(a, b)$, for each scale-time pair (a,b). In this way, the wavelet coefficients in (14) and can be seen as the outputs of a set of scaled bandpass filters. The scale factor a shifts the bandpass filters in the frequency domain, and also changes the bandwidth of the bandpass filters. Therefore, the energy of the wavelet transform of a sinusoid at a frequency ω_s will spread out

around the scale factor $a_s = \omega_\psi / \omega_s$, where ω_ψ is the center frequency of a wavelet, while the energy of the original frequency ω_s is spread across a_s. Thus, the estimated frequency present in those scales is equal to the original frequency ω_s. Consequently, the instantaneous frequency $\omega_x(a, b)$ can be estimated as

$$\omega_x(a, b) = -i W(a, b)^{-1} \frac{\partial W(a, b)}{\partial b} \qquad (15)$$

for each scale-time pair (a,b). The resulting wavelet coefficients that contain the same instantaneous frequencies can then be combined using a procedure referred to as synchrosqueezing (SST). For a set of wavelet coefficients $W(a, b)$, the synchrosqueezing transform[1] $T(\omega_l, b)$ is given by

$$T(\omega_l, b) = \sum_{a_k: \, |\omega_x(a_k, b) - \omega_l| \leq \Delta\omega/2} W(a_k, b) a^{-3/2} \, \Delta a_k \qquad (16)$$

where ω_l are the frequency bins with a resolution[2] of $\Delta\omega$. The SST has been shown to reconstruct univariate modulated oscillations of the form in (1), as follows [16]

$$x(b) = \Re \left[R_\psi^{-1} \sum_l T(\omega_l, b) \Delta\omega \right] \qquad (17)$$

where $R_\psi = \frac{1}{2} \int_0^\infty \hat{\psi}^*(\xi) \frac{d\xi}{\xi}$, is the normalization constant and $\hat{\psi}(\xi)$ is the Fourier transform of the mother wavelet $\psi(t)$.

4. Multivariate time-frequency representation using the SST

In order to extend the SST to the analysis of multivariate signals, recall that if the modulated oscillatory components are known for each channel as in (3), then we can determine the joint instantaneous frequency, provided that the frequencies of the modulated oscillations are sufficiently close together. With that insight, we propose to first partition the time-frequency domain into K frequency bands $\{\omega_k\}_{k=1,\dots,K}$. This makes it possible to identify, a set of matched monocomponent signals from a given multivariate signal. The instantaneous amplitudes and frequencies present within those frequency bands can then be determined (yielding amplitude and frequency modulated oscillations, similar to the intrinsic-mode functions (IMFs) of the EMD algorithm [18]).

4.1. Partitioning of the time-frequency domain

We propose to partition the time-frequency domain via a multivariate extension of an adaptive frequency tiling technique first proposed in [19]; the underlying concept is to determine multivariate monocomponent signals based on the multivariate bandwidth. The time-frequency plane is first partitioned into 2^l equal-width frequency bands, for the frequency range, $\omega_{l,m} = [m/2^{(l+1)}, (m+1)/2^{(l+1)}]$, where

---

[1] A detailed implementation of the synchrosqueezing transform can be found in [22].

[2] We have used linear frequency scales therefore $\Delta\omega$ is constant, however for logarithmic frequency scales, $\Delta\omega$ would vary with frequency [22].
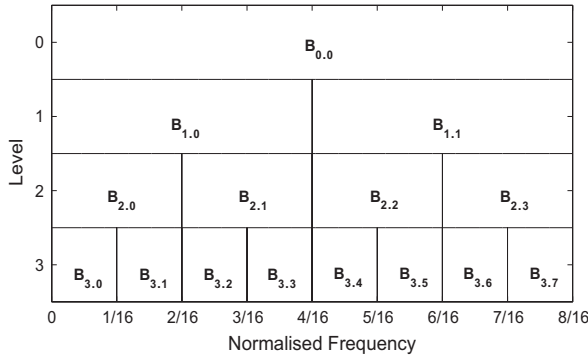
Fig. 1. The partitioned frequency domain with the multivariate bandwidth given by $\mathbf{B}_{l,m}$, where l corresponds to the level of the frequency band and m is the frequency band index.

$l = 0, \ldots, L$, corresponds to the *level* of the frequency bands ($L = 5$ typically) and $m = 0, \ldots, 2^l - 1$, is the *index* of the frequency band.

The multivariate bandwidth $\mathbf{B}_{l,m}$ for a given frequency band at level l and index m, is then calculated as shown in Fig. 1. Within a given frequency band $\omega_{l,m}$, the multivariate bandwidth is split into two frequency subbands $\omega_{l+1,2m}$ and $\omega_{l+1,2m+1}$, as follows [19]:

- If the frequency band $\omega_{l,m}$ contains a multivariate monocomponent signal, then, $\mathbf{B}_{l,m} = \mathbf{B}_{l+1,2m} + \mathbf{B}_{l+1,2m+1}$.
- If each frequency subband contains separate multivariate monocomponents then, $\mathbf{B}_{l,m} > \mathbf{B}_{l+1,2m} + \mathbf{B}_{l+1,2m+1}$.

As a result, given a multivariate signal $\mathbf{x}(t)$ with N channels with the SST coefficients for each channel given by $T_n(\omega, b)$, the multivariate bandwidth for a given frequency band $\omega_{l,m}$ [5,6], is obtained by first calculating the Fourier transform of the inverse of the SST coefficients

$$\boldsymbol{\Phi}_{l,m}(\omega) = \left[\mathcal{F} \left\{ R_\psi^{-1} \sum_{\omega \in \omega_{l,m}} T_n(\omega, b) \right\} \right]_{n=1,\ldots,N} \quad (18)$$

where $\mathcal{F}\{\cdot\}$ is the Fourier transform operator, R_ψ the normalization constant [16] and $\boldsymbol{\Phi}_{l,m}(\omega) \in \mathbb{R}^N$ a column vector. The multivariate bandwidth is then determined via Eqs. (7)–(10), as outlined in Section 2.

The rationale behind the adaptive frequency scales is then as follows: if the initial multivariate bandwidth is calculated for the entire signal at level $l = 0$, then the bandwidth is split based on the following condition:

$$\mathbf{B}_{l,m} > \frac{\mathbf{B}_{l+1,2m} \Lambda_{l+1,2m+1} + \mathbf{B}_{l+1,2m+1} \Lambda_{l+1,2m+1}}{\Lambda_{l+1,2m+1} + \Lambda_{l+1,2m+1}} \quad (19)$$

where

$$\Lambda_{l+1,2m} = \sum_{b=1}^{T} (A_{l+1,2m}^{multi}(b))^2$$

$$\Lambda_{l+1,2m+1} = \sum_{b=1}^{T} (A_{l+1,2m+1}^{multi}(b))^2$$

and $A_{l+1,2m}^{multi}(b)$ and $A_{l+1,2m+1}^{multi}(b)$ correspond to the multivariate instantaneous amplitudes for the respective frequency subbands, as defined by (23). The right hand side of (19) factors the total energy of the frequency subbands, such that the subbands with negligible signal content are not considered. The final set of adaptive frequency bands is given by $\{\omega_k\}_{k=1,\ldots,K}$, where K is the number of oscillatory scales and $\omega_1 > \omega_2 > \cdots > \omega_K$.

Remark 4. For modulated oscillations separated in frequency, the proposed partitioning method provides a robust method for separating monocomponent signals. However, for closely spaced monocomponent functions that are separated in both time and frequency (i.e. two parallel chirp signals), the method cannot resolve the separate monocomponent signals.

4.2. Multivariate time-frequency representation

For a multivariate signal $\mathbf{x}(t)$ with the corresponding SST coefficients for each channel $T_n(\omega, b)$ (the SST coefficients $T_n(\omega, b)$ have been normalized with the constant R_ψ), and a given a set of oscillatory scales $\{\omega_k\}_{k=1,\ldots K}$ obtained using a multivariate extension of a method proposed in [19], the instantaneous frequency $\Omega_k^n(b)$ for each frequency band k is given by

$$\Omega_k^n(b) = \frac{\sum_{\omega \in \omega_k} |T_n(\omega, b)|^2 \omega}{\sum_{\omega \in \omega_k} |T_n(\omega, b)|^2} \quad (20)$$

and the instantaneous amplitude $A_k^i(b)$ for each frequency band as

$$A_k^n(b) = \sqrt{\sum_{\omega \in \omega_k} |T_n(\omega, b)|^2}. \quad (21)$$

The following condition holds for the instantaneous frequencies calculated in each frequency band, $\Omega_k^n(b) > \Omega_{k-1}^n(b)$, that is, at each point in time the instantaneous frequencies are well separated. The second step is to estimate the multivariate instantaneous frequency by combining, for a given frequency band k, the instantaneous frequencies across the N channels, using the joint instantaneous frequency in (4). As a result, the multivariate instantaneous frequency band $\Omega_k^{multi}(b)$ is given by[3]

$$\Omega_k^{multi}(b) = \frac{\sum_{n=1}^{N} (A_k^n(b))^2 \Omega_k^n(b)}{\sum_{n=1}^{N} (A_k^n(b))^2} \quad (22)$$

while the instantaneous amplitude $A_k^{multi}(b)$ for each frequency band becomes

$$A_k^{multi}(b) = \sqrt{\sum_{n=1}^{N} (A_k^n(b))^2}. \quad (23)$$

Now that we have determined the joint instantaneous amplitude and frequency for each frequency band, it is possible to generate the multivariate time-frequency

---

[3] A bound on the error of the estimated multivariate instantaneous frequency is provided in the Appendix.

coefficients $\mathbf{T}_k^{multi}(\omega, b)$ for each oscillatory scale k, as[4]

$$\mathbf{T}_k^{multi}(\omega, b) = A_k^{multi}(b)\delta(\omega - \Omega_k^{multi}(b)) \qquad (24)$$

where $\delta(\cdot)$ is the Dirac delta function and the multivariate time-frequency coefficients for each oscillatory scale are given by $\mathbf{T}^{multi}(\omega, b) = \mathbf{T}_k^{multi}(\omega, b)|_{k=1,\ldots,K}$. However, it should be noted that phase information has been lost through calculating the instantaneous frequency, and so the original multivariate signal $\mathbf{x}(t)$ cannot be reconstructed. A summary of the proposed method is shown in Algorithm 1.

Algorithm 1. Multivariate extension of the SST.

1. Given a multivariate signal $\mathbf{x}(t)$ with N channels, apply the SST channel-wise in order to obtain the coefficients $T_n(\omega, b)$.
2. Determine a set of partitions along the frequency axis for the time-frequency domain, and calculate the instantaneous frequency $\Omega_k^n(b)$ and amplitude $A_k^i(b)$ for each frequency bin k, as shown in Eqs. (20) and (21) respectively.
3. Calculate the multivariate instantaneous frequency $\Omega_k^{multi}(b)$ and amplitude $A_k^{multi}(b)$ according to Eqs. (22) and (23) respectively.
4. Determine the multivariate synchrosqueezed coefficients $\mathbf{T}^{multi}(\omega, b)$.

5. Simulations

The performance of the proposed multivariate extension of the synchrosqueezed transform was evaluated on both synthetic and real-world signals. The synthetic data were of sinusoidal oscillations in varying levels of noise, as well as frequency- and amplitude- modulated oscillations in noise. The real-world simulations were conducted on velocity data collected from a freely drifting oceanographic float (used by oceanographers to analyze ocean currents) and Doppler shift signatures of a robotic device collected from two Doppler radar systems.

5.1. Sinusoidal oscillation in noise

The first set of simulations provides a quantitative evaluation the proposed multivariate time-frequency algorithm based on the synchrosqueezing transform against the multivariate pseudo Wigner distribution (MPWD) algorithm (as outlined in Appendix B). The quantitative performance index was a modification of a measure proposed in [24], given by

$$B = \frac{\int\int_{(t,\omega)\,\in\,R}|TFR(t,\omega)|\;dt d\omega}{\int\int_{(t,\omega)\,\notin\,R}|TFR(t,\omega)|\;dt d\omega} \qquad (25)$$

where the symbol $TFR(t,\omega)$ denotes the time-frequency representation, and R is the instantaneous frequency path

---

[4] The multivariate extension of the synchrosqueezed transform $\mathbf{T}^{multi}(\omega, b)$ follows a similar form to the ideal time-frequency distribution function $ITF(t,\Omega) = 2\pi|A(t)|^2\delta(\Omega - \phi'(t))$ [23].

of the desired signal. We first considered a bivariate sinusoidal oscillation in varying levels of white Gaussian noise

$$\mathbf{y}_s(t) = \begin{bmatrix} \cos(2\pi ft) \\ \cos(2\pi(f+\delta)t) \end{bmatrix} + \begin{bmatrix} n_1(t) \\ n_2(t) \end{bmatrix}$$
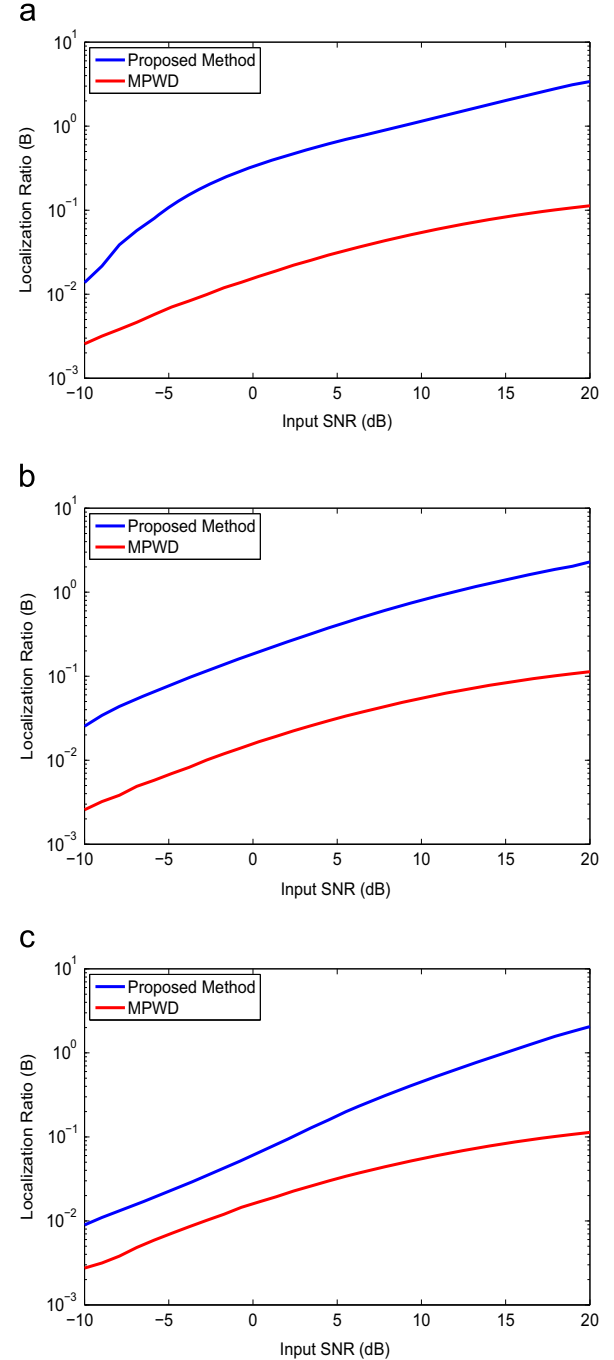

Fig. 2. A comparison between the localization ratios B, for both the proposed method and the MPWD, evaluated for a bivariate oscillation with the following joint instantaneous frequencies: (a) 10.5 Hz, (b) 40.5 Hz, and (c) 100.5 Hz. A window length of 1001 samples was used for the MPWD.

where $f = [10, 40, 100]$ Hz are the set of frequencies present, and $n_1(t)$ and $n_2(t)$ are independent white Gaussian noise realizations and $\delta = 1$ Hz corresponds to a frequency deviation between the channels. The resulting joint instantaneous frequency between the channels is given by $f_j(t) = [10.5, 40.5, 100.5]$ Hz. The values of the localization ratio B are shown in Fig. 2. It can be seen that the proposed multivariate time-frequency algorithm had a high localization ratio, as compared to the MPWD, particularly when the SNR of the input signal is relatively high. The localization ratio of the MPWD remained largely unchanged for different sinusoids, while the localization ratio for the proposed method decreases as the frequency of the sinusoid increases.
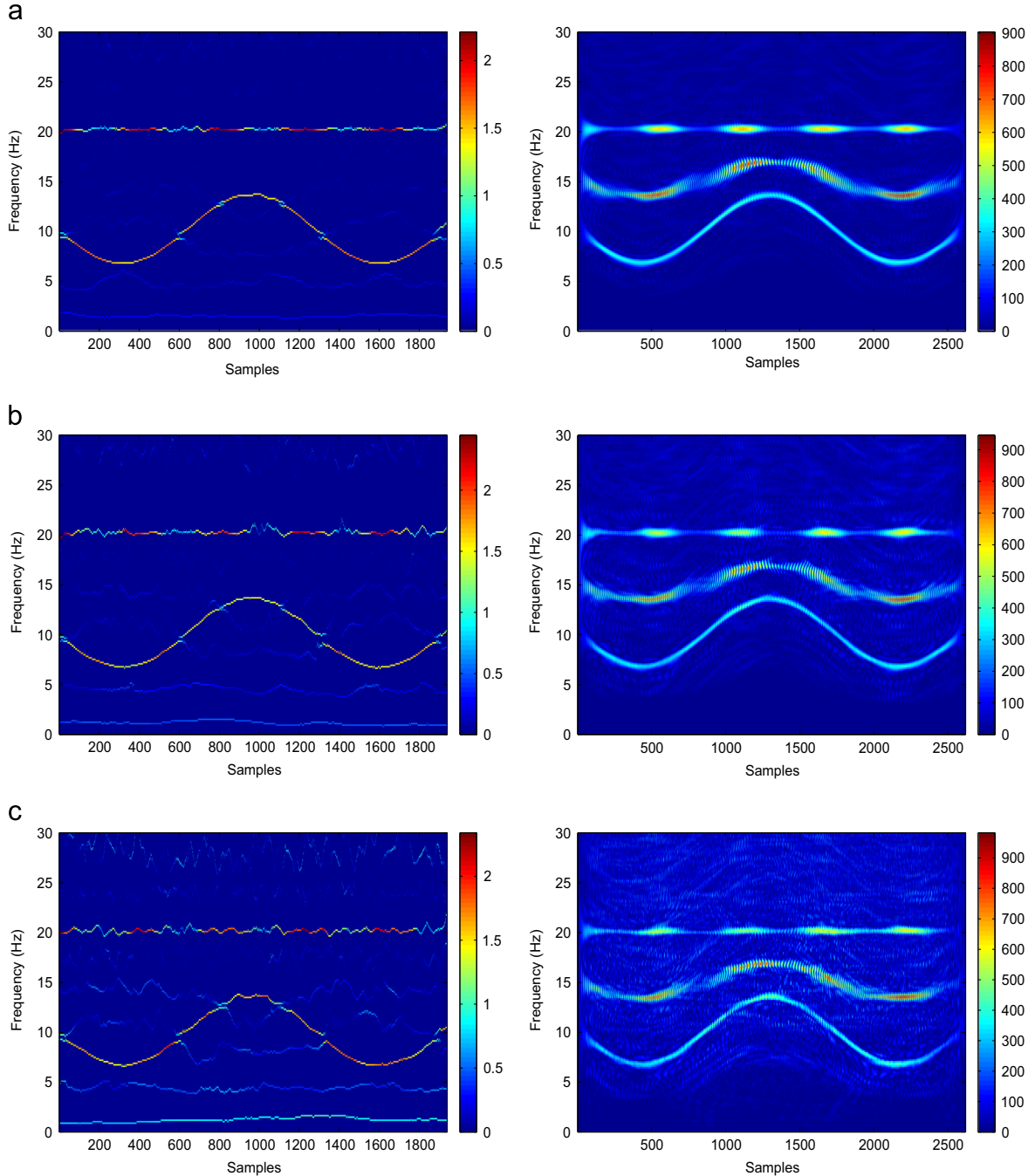

Fig. 3. The time-frequency representations for both the proposed method (left panels) and the MWPD (right panels) for a bivariate AM/FM signal, with input SNR of (a) 10 dB, (b) 5 dB and (c) 0 dB. The window length used for MPWD was 681 samples.

5.2. Amplitude and frequency modulated signal analysis

We next considered a multicomponent bivariate AM/FM signal $\mathbf{y}(t)$ corrupted by noise

$$\mathbf{y}(t) = \begin{bmatrix} s_1(t) + s_2(t) \\ s_3(t) + s_4(t) \end{bmatrix} + \begin{bmatrix} n_1(t) \\ n_2(t) \end{bmatrix}$$

where $n_1(t)$ and $n_2(t)$ are independent white Gaussian noise realizations and the signal components $s_1(t), s_2(t), s_3(t), s_4(t)$ are given by

$$s_1(t) = (1 + 0.5 \cos(2\pi t)) \cos(2\pi t 20)$$
$$s_2(t) = (1 + 0.5 \cos(2\pi t)) \cos(2\pi t (20 + \delta))$$
$$s_3(t) = \cos(2\pi(10t + 3.5 \cos(t)))$$
$$s_4(t) = \cos(2\pi((10 + \delta)t + 3.5 \cos(t))).$$

Table 1
Localization ratios, B, for both the proposed algorithm and the MPWD.

SNR (dB)	Proposed method	MPWD
10	0.208	0.037
5	0.105	0.025
0	0.04	0.014

Therefore, the components $s_1(t)$ and $s_2(t)$ were AM signals, with an amplitude modulation index of 0.5. A frequency deviation, $\delta = 0.3$ Hz, was introduced to the carrier of $s_2(t)$ (this is analogous to a frequency bias that may arise between sensors during data acquisition). The information bearing components $s_3(t)$ and $s_4(t)$ of the bivariate signal $\mathbf{y}(t)$ were sinusoidally modulated FM signals, while $s_4(t)$ also had a frequency deviation of $\delta = 0.3$ Hz.

Fig. 3 shows the time-frequency representations using both the proposed method and the MPWD, in processing the bivariate AM/FM multicomponent signal $\mathbf{y}(t)$, over a range of input SNRs. Observe from Fig. 3(a) that for an input SNR of 10 dB, that the proposed method localizes the energy of the oscillations along the instantaneous frequency frequencies that correspond to the components of $\mathbf{y}(t)$. However as the noise power increased, the performance of the proposed method degraded as the joint instantaneous frequency estimator is sensitive to noise. On the other hand, the MPWD is less localized at higher SNRs, while the performances of both methods converge for lower SNRs. Table 1 shows the localization ratio B for both techniques, illustrating that as the SNR decreases the localization ratio B for the proposed algorithm converges with that of the MPWD, implying that while localized the
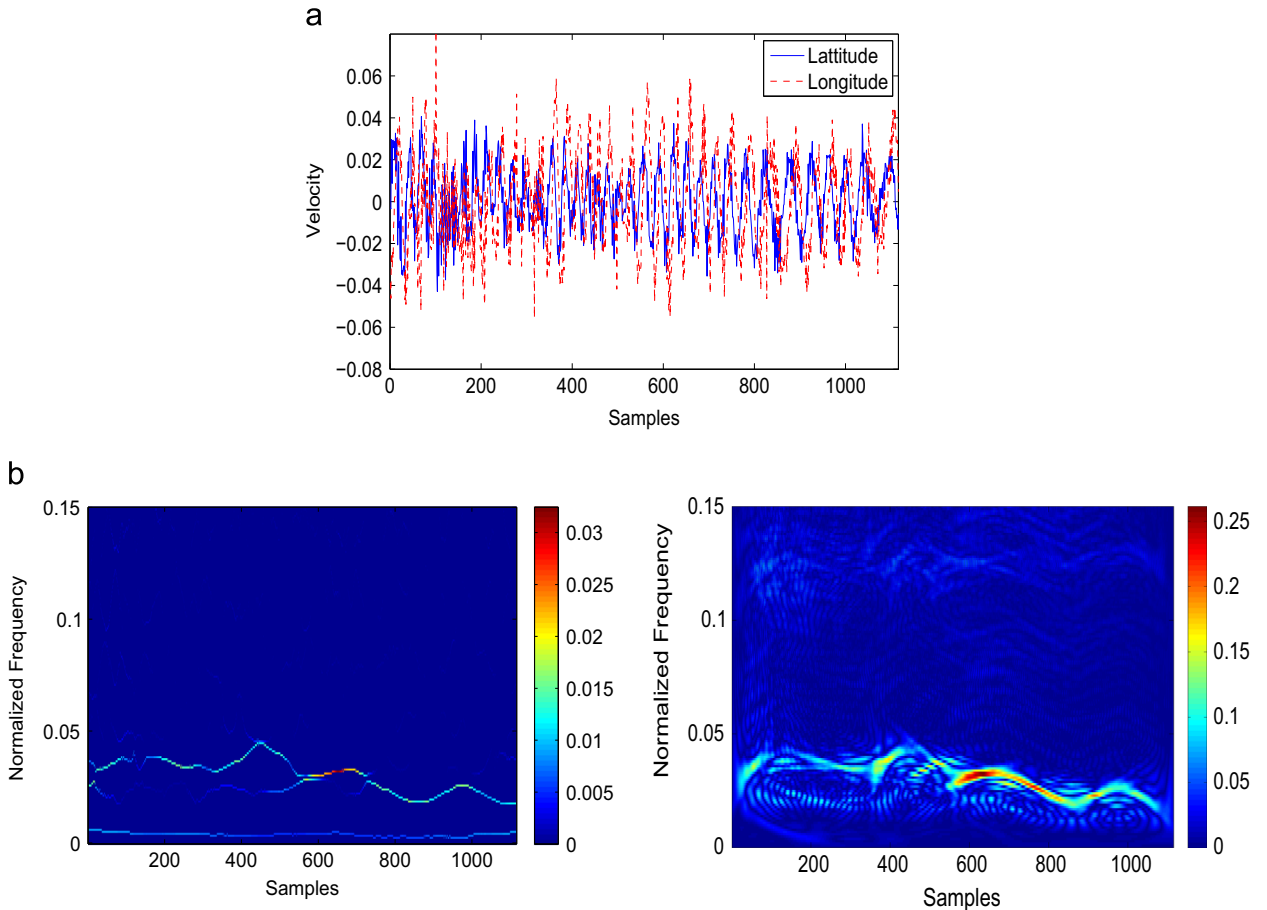

Fig. 4. Time-frequency analysis of real world float drift data. (a) The time domain waveforms of bivariate float velocity data. (b) The time-frequency representation of float data using the proposed multivariate extension of the SST (left panel) and the MPWD algorithm (right panel). A window length 501 was used for the MPWD.
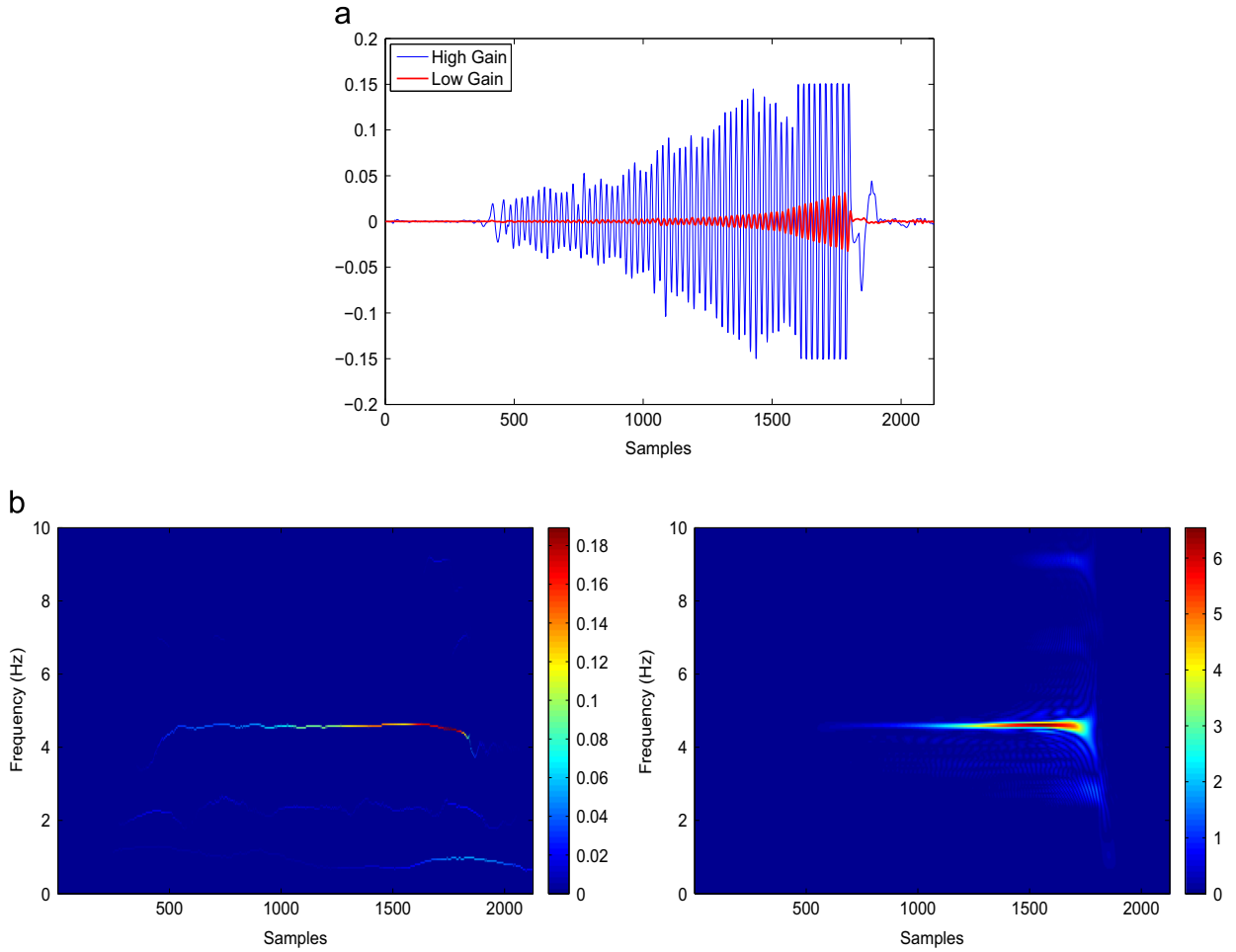
Fig. 5. Time-frequency analysis of Doppler radar data. (a) The time domain waveforms of both the high gain and low gain Doppler radar data. (b) The time-frequency representation of Doppler radar data using the proposed multivariate extension of the SST (left panel) and the MPWD algorithm (right panel). A window length 1063 was used for the MPWD.

proposed method is not accurately representing the components instantaneous frequencies.

5.3. Float drift data

The real world data was collected from a freely drifting oceanographic float, used by oceanographers to study ocean current drifts.[5] The latitude and the longitude of the float was recorded, and the resulting drift velocity in both the latitude and longitude were processed as a bivariate signal. The drift velocities along the latitude and longitude (shown in Fig. 4(a)) contain a time-varying oscillation that is common to both channels, however these oscillations are not in phase. Also the noise in both channels had different characteristics. Fig. 4(b) illustrates that the common oscillatory dynamics of the float drift data that is frequency modulated is effectively localized

using the proposed method, while the multivariate pseudo Wigner distribution had poorer localization.

5.4. Doppler speed estimation

The second real world data example consists of a bivariate Doppler radar signal, collected from both a high gain and low gain Doppler radar system (the Doppler radar operating frequency was $f_c = 10.587$ GHz). A Doppler shift signature was then collected from a robotic device moving at a constant speed towards both the high gain and low gain Doppler radars [25]. The speed chosen for this work was 0.065 m/s and the corresponding Doppler shift frequency,[6] was $f_d = 4.567$ Hz. From Fig. 5(a), observe from the output of both Doppler radar systems, the amplitude increasing as the robotic device approaches the radar. Also note that the power from the output of the high gain radar

---

[5] The float drift data was obtained from the Jlab toolbox, and is available at http://www.jmlilly.net.

[6] The Doppler shift frequency, f_d, is related to the speed of an object by $f_d = 2f_c v/c$, where v is the speed of the object and c is the speed of light.

is significantly higher than the output of the low gain radar. The multivariate time-frequency representations using both the proposed method and the MPWD is shown in Fig. 5(b). Observe that the proposed method localizes the Doppler shift frequency more effectively, where it should be noted that the speed of the robotic device between the samples 400–600, and the deceleration between the samples 1600–1800, can clearly be identified. Finally the localization ratio for the proposed multivariate time-frequency[7] method is 0.38 while for the MPWD 0.11, implying that the proposed method has a higher energy concentration around the Doppler shift frequency, f_d.

6. Conclusion

We have proposed a multivariate extension of the synchrosqueezing transform in order to identify oscillations common to the data channels within a multivariate signal. For each channel, the instantaneous frequencies of the synchrosqueezed coefficients are determined for each oscillatory scale, and the resulting multivariate instantaneous frequency is then found by calculating the joint instantaneous frequency of each oscillatory scale across the channels. The performance of the proposed algorithm has been illustrated both analytically, in terms of an error bound, and through simulations on synthetic and real-world signals. Finally, while the algorithm has shown potential in generating a localized multivariate time-frequency representation, further work is required for the operation in highly noisy environments.

Appendix A

This Appendix presents a bound on the error of the multivariate instantaneous frequency estimate $\hat{\Omega}_{multi}(b)$ (shown in (20)), based on error bounds for the univariate synchrosqueezing transform [16]. We first present a brief overview of the main results presented in [16] and proceed to derive a bound for the estimated multivariate instantaneous frequency.

A real-valued oscillatory function of the form $f(t) = A(t) \cos(\phi(t))$, can be considered an intrinsic mode type (IMT) function, with accuracy ϵ, if the following conditions on A and ϕ hold

$$A \in C^1(\mathbb{R}) \cap L_\infty(\mathbb{R}), \quad \phi \in C^2(\mathbb{R})$$
$$\inf_{t \in \mathbb{R}} \phi'(t) > 0, \quad \sup_{t \in \mathbb{R}} \phi'(t) < \infty$$
$$|A'(t)|, |\phi''(t)| \le \epsilon |\phi'(t)|, \quad \forall t \in \mathbb{R}$$

A signal $f(t)$ that satisfies the above constraints, has its corresponding wavelet transform given by $W_f(a, b)$, and

the Fourier transform of the wavelet function $\hat{\psi}$ having a compact support in $[1-\Delta, 1+\Delta]$. The synchrosqueezing transform with accuracy δ and threshold $\tilde{\epsilon}$ (where $\tilde{\epsilon} = \epsilon^{-1/3}$ is the threshold for which $|W_f(a,b)| > \tilde{\epsilon}$) is then determined via [16]

$$S_{f,\tilde{\epsilon}}^\delta(b, \omega) = \int_{a:|W_f(a,b)| > \tilde{\epsilon}} W_f(a,b) \frac{1}{\delta} h\left(\frac{\omega - \omega_f(a,b)}{\delta}\right) a^{-3/2} \, da \tag{26}$$

where $h(t)$ is a window function which satisfies, $\int h(t) \, dt = 1$. The following error bounds have been determined in [16]

- Given a scale band $Z = \{(a, b): |a\phi'(b) - 1| < \Delta\}$, then for each scale-time pair $(a, b) \in Z$ and $|W_f(a, b)| > \tilde{\epsilon}$, it follows that

$$|\omega_f(a, b) - \phi'(b)| \le \tilde{\epsilon}, \tag{27}$$

  which implies that the SST coefficients are concentrated along the instantaneous frequency $\phi'(b)$.
- For all of $b \in \mathbb{R}$, there exists a constant C, such that as $\delta \to 0$, the inverse of the synchrosqueezing transform along the vicinity of the instantaneous frequency curve, $\phi'(b)$, results in the following error bound:

$$\left| \lim_{\delta \to 0} \left(\frac{1}{R_\psi} \int_{\omega:|\omega - \omega_f(a,b)| < \tilde{\epsilon}} S_{f,\tilde{\epsilon}}^\delta(b, \omega) \, d\omega \right) - A(b) e^{i\phi(b)} \right| \le C\tilde{\epsilon} \tag{28}$$

The multivariate instantaneous frequency estimate is then the power weighted average of the instantaneous amplitudes and frequencies of the multivariate signal according to (4). Therefore, a bound on the error of the multivariate instantaneous frequency depends upon the channel-wise errors when estimating the instantaneous amplitude and frequency of a modulated oscillation using the synchrosqueezed transform. Based upon the univariate SST error bounds with the instantaneous frequency $\phi'_n(b)$ and amplitude $A_n(b)$ (where n is the channel index) and scale bands for each channel given by $Z_n = \{(a, b): |a\phi'_n(b) - 1| < \Delta\}$, with $|W_n(a, b)| > \tilde{\epsilon}$, the instantaneous frequency for each channel is bounded by

$$\phi'_n(b) - \tilde{\epsilon} \le \omega_n(a, b) \le \phi'_n(b) + \tilde{\epsilon} \tag{29}$$

with the bound on the corresponding error bound for the instantaneous amplitude, obeying

$$A_n(b) - C\tilde{\epsilon} < \hat{A}_n(b) < A_n(b) + C\tilde{\epsilon} \tag{30}$$

where

$$\hat{A}_n(b) = \left| \lim_{\delta \to 0} \left(\frac{1}{R_\psi} \int_{\omega:|\omega - \omega_n(a,b)| < \tilde{\epsilon}} S_{f,\tilde{\epsilon},n}^\delta(b, \omega) \, d\omega \right) \right|.$$

For the estimate of the multivariate instantaneous frequency (determined using (22)), the objective is to determine an error bound on $|\hat{\Omega}_{multi}(b) - \Omega_{multi}(b)|$, in the form:

$$|\hat{\Omega}_{multi}(b) - \Omega_{multi}(b)| = \left| \frac{\sum_{n=1}^N \hat{A}_n^2(b) \omega_n(a, b)}{\sum_{n=1}^N \hat{A}_n^2(b)} - \Omega_{multi}(b) \right|$$

---

[7] It should be noted that the localization ratio of the proposed method and the univariate SST of the high gain channel are equal, as the instantaneous frequency of interest in both cases is $f_d = 4.567$ Hz.

$$= \left| \frac{\sum_{n=1}^{N} \hat{A}_n^2(b)(\omega_n(a,b) - \Omega_{multi}(b))}{\sum_{n=1}^{N} \hat{A}_n^2(b)} \right|. \tag{31}$$

Using the following property, $|\sum_{n=1}^{N} y_n| \le \sum_{n=1}^{N} |y_n|$, Eq. (31) can be written as follows:

$$\left| \frac{\sum_{n=1}^{N} \hat{A}_n^2(b)(\omega_n(a,b) - \Omega_{multi}(b))}{\sum_{n=1}^{N} \hat{A}_n^2(b)} \right|$$

$$< \sum_{n=1}^{N} \left| \frac{\hat{A}_n^2(b)(\omega_n(a,b) - \Omega_{multi}(b))}{A_{lower}^2} \right|$$

$$= \sum_{n=1}^{N} \left| \frac{\hat{A}_n^2(b)}{A_{lower}^2} \right| \left| \frac{(\omega_n(a,b) - \Omega_{multi}(b))}{A_{lower}^2} \right|.$$

where $A_{lower}^2 = \sum_{n=1}^{N} (A_n(b) - C\tilde{\epsilon})^2$. Finally, using inequalities (30) and (29), we have

$$\sum_{n=1}^{N} \left| \frac{\hat{A}_n^2(b)}{A_{lower}^2} \right| \left| \frac{(\omega_n(a,b) - \Omega_{multi}(b))}{A_{lower}^2} \right|$$

$$< \sum_{n=1}^{N} \left| \frac{(A_n(b) + C\tilde{\epsilon})^2}{A_{lower}^2} \right| \left| \frac{(\phi_n'(b) - \Omega_{multi}(b) + \tilde{\epsilon})}{A_{lower}^2} \right| \tag{32}$$

Therefore, the error bound in (32) is dependent upon the differences of the individual channel-wise instantaneous frequencies from the calculated multivariate instantaneous frequency. However, if the instantaneous frequencies within each channel are equal, from (32) this implies that the bound is a multiple of the threshold $\tilde{\epsilon}$.

Appendix B

This Appendix derives a multivariate extension for the Wigner distribution which naturally estimates the joint instantaneous frequency for a multivariate signal. Given a multivariate analytic signal $\mathbf{x}_+(t)$, the Wigner distribution is defined by

$$WD(\omega, t) = \int_{-\infty}^{\infty} \mathbf{x}_+^H \left(t - \frac{\tau}{2} \right) \mathbf{x}_+ \left(t + \frac{\tau}{2} \right) e^{-j\omega\tau} \, d\tau. \tag{33}$$

and its inverse as

$$\mathbf{x}_+^H \left(t - \frac{\tau}{2} \right) \mathbf{x}_+ \left(t + \frac{\tau}{2} \right) = \frac{1}{2\pi} \int_{-\infty}^{\infty} WD(\omega, t) e^{j\omega\tau} \, d\omega$$

where $\mathbf{x}_+^H(t)$ is the Hermitian transpose of a vector $\mathbf{x}_+(t)$ defined in (3).

The central frequency of the Wigner distribution of a multivariate signal $\mathbf{x}_+(t)$, for a given instant t, is given by

$$\langle \omega(t) \rangle = \frac{\int_{-\infty}^{\infty} \omega WD(\omega, t) \, d\omega}{\int_{-\infty}^{\infty} WD(\omega, t) \, d\omega}. \tag{34}$$

Using the inverse Wigner distribution we can now rewrite (34) as

$$\langle \omega(t) \rangle = \frac{\frac{d}{jd\tau} \left[\mathbf{x}_+^H \left(t - \frac{\tau}{2} \right) \mathbf{x}_+ \left(t + \frac{\tau}{2} \right) \right]_{|\tau=0}}{\mathbf{x}_+^H \left(t - \frac{\tau}{2} \right) \mathbf{x}_+ \left(t + \frac{\tau}{2} \right)_{|\tau=0}}$$

$$= \frac{1}{2j} \frac{[\mathbf{x}_+^H(t)\mathbf{x}_+'(t) - \mathbf{x}_+'^H(t)\mathbf{x}_+(t)]}{\mathbf{x}_+^H(t)\mathbf{x}_+(t)}.$$

For the multivariate signal components $x_n(t) = a_n(t)e^{i\phi_n(t)}$, the instantaneous frequency of a multivariate signal is therefore of the form

$$\langle \omega(t) \rangle = \frac{\sum_{n=1}^{N} a_n^2(t)\phi_n'(t)}{\sum_{n=1}^{N} a_n^2(t)} = \omega_x(t).$$

In a similar way, the instantaneous bandwidth (4) follows from

$$v_x^2(t) = \frac{\int_{-\infty}^{\infty} (\omega - \omega_x(t))^2 WD(\omega, t) \, d\omega}{\int_{-\infty}^{\infty} WD(\omega, t) \, d\omega}$$

with

$$\frac{1}{2\pi} \int_{-\infty}^{\infty} \omega^2 WD(\omega, t) \, d\omega = -\frac{d^2}{d\tau^2} \left[\mathbf{x}_+^H \left(t - \frac{\tau}{2} \right) \mathbf{x}_+ \left(t + \frac{\tau}{2} \right) \right]_{|\tau=0}.$$

This analysis can be generalized to the Cohen class of distributions and general time-scale representations, including the spectrogram and the scalogram as the energetic forms of the short-time Fourier transform and the wavelet transform, respectively [26]. Finally, in order to implement the MWD, we used an multivariate extension of the pseudo Wigner distribution [23], where a window function is used to evaluate (33).

References

[1] D. Gabor, Theory of communication, Proc. IEEE 93 (1946) 429–457.
[2] B. Picinbono, On instantaneous amplitude and phase of signals, IEEE Trans. Signal Process. 45 (3) (1997) 552–560.
[3] C. Park, D. Looney, N. Rehman, A. Ahrabian, D.P. Mandic, Classification of motor imagery BCI using multivariate empirical mode decomposition, IEEE Trans. Neural Syst. Rehabil. Eng. 21 (1) (2013) 10–22.
[4] L. Stanković, Time-frequency distributions with complex argument, IEEE Trans. Signal Process. 50 (3) (2002) 475–486.
[5] J.M. Lilly, S.C. Olhede, Bivariate instantaneous frequency and bandwidth, IEEE Trans. Signal Process. 58 (2) (2010) 591–603.
[6] J.M. Lilly, Modulated oscillations in three dimensions, IEEE Trans. Signal Process. 59 (12) (2011) 5930–5943.
[7] J. Lilly, R. Scott, S. Olhede, Extracting waves and vortices from Lagrangian trajectories, Geophys. Res. Lett. 38 (23) (2011) 1–5.
[8] J.M. Lilly, S.C. Olhede, Wavelet ridge estimation of jointly modulated multivariate oscillations, in: 2009 Conference Record of the Forty-Third Asilomar Conference on Signals, Systems and Computers, 2009, pp. 452–456.
[9] J.M. Lilly, S.C. Olhede, Analysis of modulated multivariate oscillations, IEEE Trans. Signal Process. 60 (2) (2012) 600–612.
[10] N. Rehman, D.P. Mandic, Multivariate empirical mode decomposition, Proc. R. Soc. A 466 (2117) (2010) 1291–1302.
[11] N. Rehman, D.P. Mandic, Filter bank property of multivariate empirical mode decomposition, IEEE Trans. Signal Process. 59 (2011) 2421–2426.
[12] K. Kodera, R. Gendrin, C. Villedary, Analysis of time-varying signals with small BT values, IEEE Trans. Acoust. Speech Signal Process. 26 (1) (1978) 64–76.
[13] F. Auger, P. Flandrin, Improving the readability of time-frequency and time-scale representations by the reassignment method, IEEE Trans. Signal Process. 43 (5) (1995) 1068–1089.

[14] F. Auger, P. Flandrin, Y.-T. Lin, S. McLaughlin, S. Meignen, T. Oberlin, H.-T. Wu, Time-frequency reassignment and synchrosqueezing: an overview, IEEE Signal Process. Mag. 30 (6) (2013) 32–41.

[15] R. Carmona, W.-L. Hwang, B. Torrésani, Practical Time-Frequency Analysis, Academic Press, 1998.

[16] I. Daubechies, J. Lu, H.-T. Wu, Synchrosqueezed wavelet transforms: an empirical mode decomposition-like tool, Appl. Comput. Harmonic Anal. 30 (2) (2011) 243–261.

[17] I. Daubechies, S. Maes, A nonlinear squeezing of the continuous wavelet transform based on auditory nerve models, in: Wavelets in Medicine and Biology, CRC Press, 1996, pp. 527–546.

[18] N. Huang, Z. Shen, S. Long, M. Wu, H. Shih, Q. Zheng, N. Yen, C. Tung, H. Liu, The empirical mode decomposition and the Hilbert spectrum for nonlinear and non-stationary time series analysis, Proc. R. Soc. A 454 (1998) 903–995.

[19] S. Olhede, A. Walden, The Hilbert spectrum via wavelet projections, Proc. R. Soc. A 460 (2004) 955–975.

[20] P. Loughlin, B. Tacer, Comments on the interpretation of instantaneous frequency, IEEE Signal Process. Lett. 4 (5) (1997) 123–125.

[21] P. Loughlin, K. Davidson, Modified Cohen–Lee time-frequency distributions and instantaneous bandwidth of multicomponent signals, IEEE Trans. Signal Process. 49 (6) (2001) 1153–1165.

[22] G. Thakur, E. Brevdo, N.S. Fuckar, H.-T. Wu, The synchrosqueezing algorithm for time-varying spectral analysis: robustness properties and new paleoclimate applications, Signal Process. 93 (5) (2013) 1079–1094.

[23] L. Stanković, M. Daković, T. Thayaparan, Time-Frequency Signal Analysis with Applications, Artech House, 2013.

[24] I. Djurovic, L. Stankovic, Time-frequency representation based on the reassigned s-method, Signal Process. 77 (1) (1999) 115–120.

[25] D. Mandic, N. Rehman, Z. Wu, N. Huang, Empirical mode decomposition-based time-frequency analysis of multivariate signals: the power of adaptive data analysis, IEEE Signal Process. Mag. 30 (6) (2013) 74–86.

[26] V. Ivanovic, M. Dakovic, L. Stankovic, Performance of quadratic time-frequency distributions as instantaneous frequency estimators, IEEE Trans. Signal Process. 51 (1) (2003) 77–89.